

Computerized “drag-and-drop” alignment of GPC-based optical micromanipulation system

Jeppe Seidelin Dam, Peter John Rodrigo, Ivan R. Perch-Nielsen, Carlo Amadeo Alonzo
and Jesper Glückstad

Optics and Plasma Research Department, Risø National Laboratory, DK-4000 Roskilde, Denmark
<http://www.ppo.dk>
jesper.gluckstad@risoe.dk

Abstract: In the past, aligning the counterpropagating beams in our 3D real-time generalized phase contrast (GPC) trapping system has been a task requiring moderate skills and prior experience with optical instrumentation. A ray transfer matrix analysis and computer-controlled actuation of mirrors, objective, and sample stage has made this process user friendly. The alignment procedure can now be done in a very short time with just a few drag-and-drop tasks in the user-interface. The future inclusion of an image recognition algorithm will allow the alignment process to be executed completely without any user interaction. An automated sample loading tray with a loading precision of a few microns has also been added to simplify the switching of samples under study. These enhancements have significantly reduced the level of skill and experience required to operate the system, thus making the GPC-based micromanipulation system more accessible to people with little or no technical expertise in optics.

©2007 Optical Society of America

OCIS codes: (170.4520) Optical confinement and manipulation; (140.7010) Trapping; (220.1140) Alignment

References and links

1. A. Ashkin, “Acceleration and trapping of particles by radiation pressure,” *Phys. Rev. Lett.* **24**, 156-159 (1970).
2. D. G. Grier, “A revolution in optical manipulation,” *Nature* **424**, 810-816 (2003).
3. J. Glückstad, “Sorting particles with light,” *Nature Materials* **3**, 9-10 (2004).
4. A. Constable, J. Kim, J. Mervis, F. Zarinetchi, and M. Prentiss, “Demonstration of a fiber-optical light-force trap,” *Opt. Lett.* **18**, 1867-1869 (1993).
5. E. R. Lyons and G. J. Sonek, “Confinement and bistability in a tapered hemispherically lensed optical fiber trap,” *Appl. Phys. Lett.* **66**, 1584-1586 (1995).
6. P. J. Rodrigo, V. R. Daria, and J. Glückstad, “Four-dimensional optical manipulation of colloidal particles,” *Appl. Phys. Lett.* **86**, 074103 (2005).
7. P. Kraikivski, B. Pouligny, and R. Dimova, “Implementing both short- and long-working-distance optical trappings into a commercial microscope,” *Rev. Sci. Instrum.* **77**, 113703 (2006).
8. P. J. Rodrigo, I. R. Perch-Nielsen, C. A. Alonzo, and J. Glückstad, “GPC-based optical micromanipulation in 3D real-time using a single spatial light modulator,” *Opt. Express* **14**, 13107-13112 (2006).
9. J. Glückstad and P. C. Mogensén, “Optimal phase contrast in common-path interferometry,” *Appl. Opt.* **40**, 268-282 (2001).
10. I. R. Perch-Nielsen, P. J. Rodrigo, and J. Glückstad, “Real-time interactive 3D manipulation of particles viewed in two orthogonal observation planes,” *Opt. Express* **13**, 2852-2857 (2005).
11. A. Ashkin, J. M. Dziedzic, J. E. Bjorkholm, and S. Chu, “Observation of a single-beam gradient force optical trap for dielectric particles,” *Opt. Lett.* **11**, 288-290 (1986).
12. P. J. Rodrigo, I. R. Perch-Nielsen, and J. Glückstad, “Three-dimensional forces in GPC-based counterpropagating-beam traps,” *Opt. Express* **14**, 5812-5822 (2006).
13. I. R. Perch-Nielsen, P. J. Rodrigo, C. A. Alonzo, and J. Glückstad, “Autonomous and 3D real-time multi-beam manipulation in a microfluidic environment,” *Opt. Express* **14**, 12199-12205 (2006).

1. Introduction

Tiny objects at the scale of a few nanometers up to tens of microns can be trapped, manipulated and even sorted by light-matter interaction [1-3]. One way to achieve optical trapping is by utilizing counterpropagating beams (CB) [4-7]. Using a single computer programmable spatial light modulator, we have previously demonstrated a real-time 3D system that can create multiple independently moveable CB traps to manipulate a plurality of objects simultaneously [8].

The generalized phase contrast (GPC) method [9] is advantageous for the synthesis of multiple optical traps by its energy-efficient means of producing intensity patterns with arbitrary numerical aperture (NA) [10]. This is not the case for the more widely applied trapping method, the gradient force optical trap [11]. The gradient trap geometry is inherently constrained to a relatively small field of view, and a narrow working distance due to the necessary use of a high-NA (oil or water immersion) focusing objective lens. However, gradient trapping systems have the advantage of relatively simpler optical alignment.

A major issue in having an array of CB traps is that the beams must be aligned to a high precision. If the axes of a pair of counterpropagating beams are relatively displaced, the optical trap will not function as intended. The target object may only sense one beam and thus be pushed along the beam axis. In addition, the beams must also have the same tilt angle. Otherwise, a CB trap may only work in a smaller region where the beams overlap. These alignment issues are illustrated in Fig. 1. A slight displacement of counterpropagating beams can create a situation, where a tiny object can be captured by the light, but spatially fixed trapping is not possible. In such a case the object will be continuously moving, as sketched in Fig. 2.

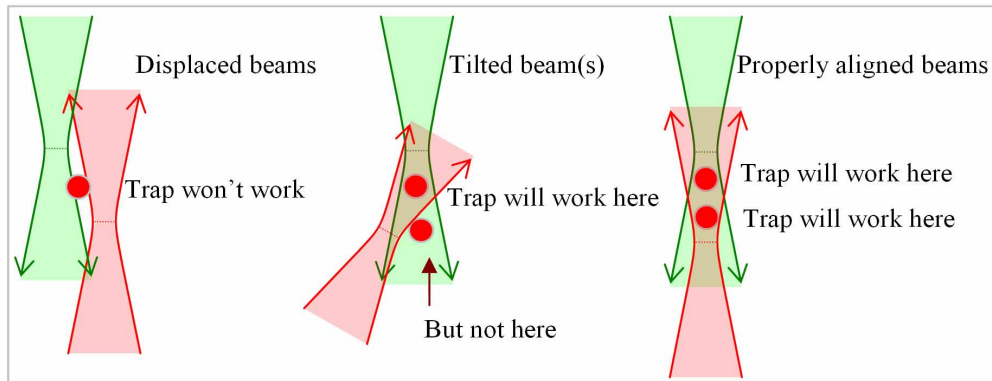


Fig. 1. To achieve stable trapping in a set of counterpropagating beams both spatial positioning and beam tilt must be addressed. Arrows indicate the propagation directions of beams.

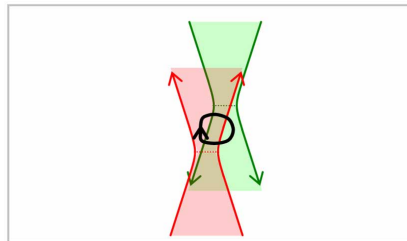


Fig. 2. Misalignment of a pair of counterpropagating beams results in a trap without a stable fix point as sketched above. An object is first trapped in one beam, pushed out of focus, trapped by the other beam, and pushed back in a looping motion. Arrows indicate the propagation directions of beams.

Finally, the separation of focal planes of the counterpropagating beams to form stable traps also depends on the size of the particles. This requirement, along with the alignment issues are major challenges in applying techniques based on CB traps [8, 12]. In this paper, we present a computer-controlled method to align the CB traps and adjust the separation of focal planes which is so simple that it can be quickly carried out without any technical expertise in optics. We further describe how making the alignment completely automatic will be quite simple. We have also implemented an automated sample loading system that eliminates direct user interaction with the system hardware. Through these enhancements, we gain increased stability of the optical system while also reducing the user's risk of exposure to laser radiation.

In the following section the effects of tilting each motorized mirror mount in the system are derived. Calculations showing how beam tilt and image translation can be separated are also demonstrated. Section 3 describes how this separation is helpful in constructing a swift and easy beam alignment procedure. Section 4 outlines an automated sample loading system allowing the user to change samples at a safe and convenient distance from the optical beam path.

2. Beam path analysis - effects of moving individual mirrors

Our experimental setup described in detail elsewhere [8] is shown in Fig. 3. The setup has been modified to include four motorized mirrors (the mirrors after the beam splitter) each of which can be tilted on two axes. For the current setup, we use computer-controlled kinematic mounts (Thorlabs KM100-Z6) to tilt the mirrors.

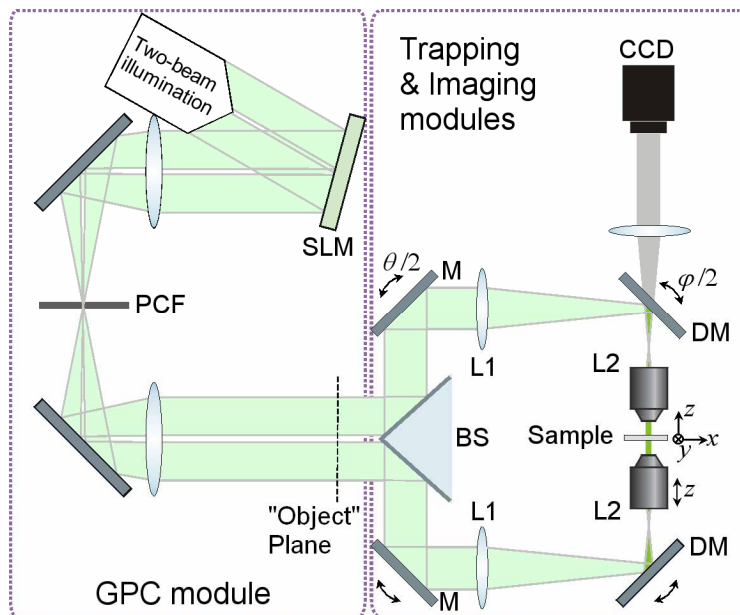


Fig. 3. The setup described in detail in our previous paper [8] has been modified with four motorized mirror mounts (mirrors marked M and DM). Tilting a mirror an angle $\theta/2$ tilts the reflected beam an angle θ . Furthermore, the lower objective has been mounted on a computer-controlled stage, and the sample stage is also computer-controlled on an x, y, z stage. Lenses marked L1 are achromatic with focal lengths (f_1) 400 mm. Objectives marked L2 are long working distance objectives with 50x magnification (NA = 0.55, focal lengths (f_2) 3.6 mm).

We have devised a procedure to align the beams based on separation of beam tilt and beam position (described in section 3). To achieve this separation the ideal situation would be to have one mirror positioned in the Fourier plane, and one mirror positioned in the "object"

plane as shown in Fig. 4. Tilting a mirror placed in the “object” plane effectively introduces beam tilt (but no displacement) in the image plane, as indicated by the green line. Tilting a mirror placed in the Fourier plane produces a beam displacement, but does not affect beam tilt in the image plane at the sample (red line).

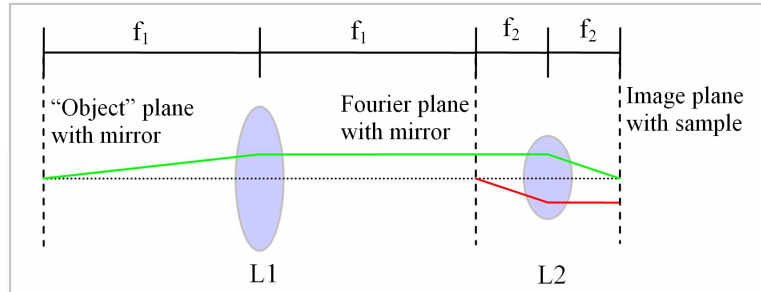


Fig. 4. In the ideal geometry for beam alignment, kinematic mirror mounts should be positioned at the “object” plane and at the Fourier plane in a 4-f setup. Tilting a mirror placed in the “object” plane will introduce tilt at the image plane. Adjusting a mirror placed in the Fourier plane results in a translation at the image plane.

However, the placement of motorized mirror mounts is constrained by the geometry of our setup depicted in Fig. 3. We cannot insert mirrors directly at the “object” and Fourier planes, but can still independently control image displacement and beam tilt by moving the two mirrors in tandem. Concurrent control of the mirror pair is simplified with the aid of a computer.

Tilting a mirror at an arbitrary position in the optical path will simultaneously introduce an amount of translation of the image and change the final tilt of the beam. A second mirror sitting at a different position will introduce different amounts of tilt and translation. By carefully choosing the ratios of mirror movements one can effectively translate the image without introducing tilt, or alternatively change the tilt without translating the image (Fig. 5). The decoupling of image translation and tilt adjustment simplifies the alignment procedure greatly.

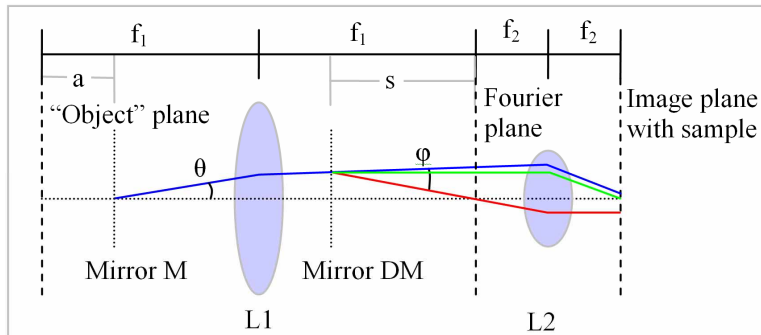


Fig. 5. Tilting “Mirror M” alone produces the blue beam path (both tilt and displacement in the image plane at the sample), but if “Mirror DM” is accordingly adjusted one can obtain either the green beam path, where the beam hits the original target with an altered tilt, or “Mirror DM” can be adjusted resulting in the beam following the red path, where no beam tilt is induced, but only a displacement of it. All angles and displacements are exaggerated for clarity.

In the following, we will calculate the ratios by which the two mirrors must be moved to independently translate the image and induce beam tilt, respectively. All calculations are carried out within the so called ‘small angle approximation’ where $\tan i \approx \sin i \approx i$, which is a

reasonable assumption for the tiny corrections applied in the alignment procedure of this work.

Using ray transfer matrix notation to calculate the effect of tilting the beam an angle (θ) with mirror M a distance a from the “object” plane, we get the following displacement and tilt at the sample image plane:

$$\begin{pmatrix} 1 & f_2 \\ 0 & 1 \end{pmatrix} \begin{pmatrix} 1 & 0 \\ -\frac{1}{f_2} & 1 \end{pmatrix} \begin{pmatrix} 1 & f_1 + f_2 \\ 0 & 1 \end{pmatrix} \begin{pmatrix} 1 & 0 \\ -\frac{1}{f_1} & 1 \end{pmatrix} \begin{pmatrix} 1 & f_1 - a \\ 0 & 1 \end{pmatrix} \begin{pmatrix} 0 \\ \theta \end{pmatrix} = \begin{pmatrix} \frac{af_2\theta}{f_1} \\ -\frac{f_1\theta}{f_2} \end{pmatrix} \quad (1)$$

A tilt (φ) introduced at the position of mirror DM (distance s from the Fourier plane), results in the following translation and tilt at the sample image plane:

$$\begin{pmatrix} 1 & f_2 \\ 0 & 1 \end{pmatrix} \begin{pmatrix} 1 & 0 \\ -\frac{1}{f_2} & 1 \end{pmatrix} \begin{pmatrix} 1 & s + f_2 \\ 0 & 1 \end{pmatrix} \begin{pmatrix} 0 \\ \varphi \end{pmatrix} = \begin{pmatrix} f_2\varphi \\ -\frac{s\varphi}{f_2} \end{pmatrix} \quad (2)$$

Accordingly, a tilt of both mirrors (θ and φ) gives the following displacement (x) and tilt (ψ) [by superposition of Eq. (1) and Eq. (2)]:

$$\begin{pmatrix} x \\ \psi \end{pmatrix} = \begin{pmatrix} \frac{af_2\theta}{f_1} \\ -\frac{f_1\theta}{f_2} \end{pmatrix} + \begin{pmatrix} f_2\varphi \\ -\frac{s\varphi}{f_2} \end{pmatrix} \quad (3)$$

Requiring $\psi=0$ in Eq. (3) for a pure translation of the image at the sample plane we derive the mirror adjustments necessary for a given displacement (x):

$$\theta(x) = \frac{-sxf_1}{f_2(f_1^2 - sa)}, \quad \varphi(x) = \frac{f_1^2 x}{f_2(f_1^2 - sa)} \quad (4)$$

Similarly, requiring $x=0$ (changing tilt without translating the image) in Eq. (3) leads to the following mirror adjustments to produce a given tilt (ψ):

$$\theta(\psi) = \frac{\psi f_2 f_1}{f_1^2 + sa}, \quad \varphi(\psi) = \frac{a\psi f_2}{f_1^2 + sa} \quad (5)$$

The equations above have rotational symmetry, and one must remember that the tilt and position alignments are undertaken in two dimensions, meaning that tilt and image translation are decomposed in x and y components when adjusting the mirrors. The ability to change image position and tilt separately is particularly valuable when aligning counterpropagating beam sets. In the next section we show how this separation along with motor control of objective and sample stage can be used to achieve perfect alignment.

3. Procedure for aligning counterpropagating beams

As shown in the previous section, moving two mirrors simultaneously, can either translate the image without introducing additional tilt or *vice versa*. This is applicable to both the upper and the lower beam sets. The alignment procedure is divided so that we first align the top beam set, and then the bottom beam set.

The top beam set is imaged using reflection from the upper glass surface of the sample chamber. By placing the glass surface exactly in the image plane, the reflection is displayed as a sharp image on the camera viewing from the top (CCD in Fig. 3). This reflected image is then centered on the screen. The image centering is done by computer mouse control. The

user simply drags a beam pattern to the center of the captured video image shown on the screen while the computer adjusts the two mirrors according to Eq. (4).

Displacing the sample downwards (by $\sim 150 \mu\text{m}$) suitably defocuses the observed image. If the projected beam pattern is not perpendicular to the sample surface (which must be completely level by design), the defocused image is no longer centered. By changing the tilt of the beam pattern, we can center the image. Again, this is done by a computer mouse drag-and-drop procedure. Now, the beam pattern is positioned in the middle of the camera view, and is perpendicular to the sample chamber. These steps are outlined in Fig. 6.

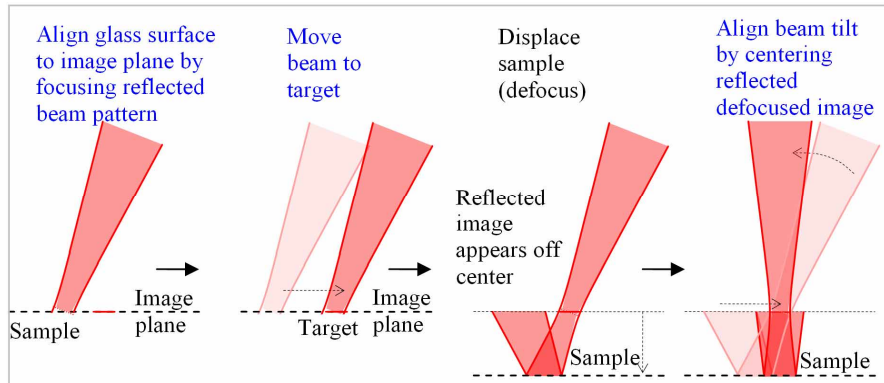


Fig. 6. The user is guided through the calibration scheme sketched above. The user is asked to click a “next” button when each step is completed to his or her satisfaction. The computer readsies for the next step in the alignment procedure. The text in blue indicates actions presently requiring user attention, whereas the black text (here axial displacement of sample) is automatically taken care of, when the user clicks “next” in the graphical user interface (GUI).

A similar procedure is followed to focus the beam pattern coming from below. For the lower beam pattern, the image is focused (and defocused) by moving the lower objective down by $200 \mu\text{m}$ (moving the sample has obviously no effect, since we are observing the transmitted beam).

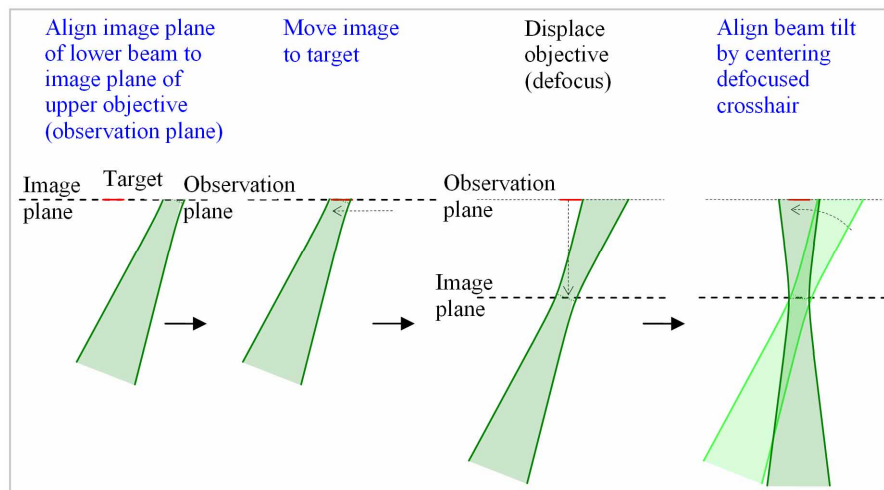


Fig. 7. Once the top beam has been aligned; the computer turns off the top beam and turns on the beam coming from below, and guides the user in going through the steps sketched above. The text in blue indicates actions presently requiring user attention, whereas the black text (here defocusing of objective) is automatically taken care of, as the user clicks “next” in the graphical user interface (GUI).

In the alignment procedure, the user is heavily assisted by a computer GUI. The computer moves the appropriate mirrors to achieve the required image displacement or beam tilt as the mouse is used to drag an image to the center position. A further benefit from using mouse control is that both x and y axes are aligned in a single user operation. A video showing the top beam being aligned by the user in real-time within 20 seconds is available online. A few frames are shown in Fig. 8.

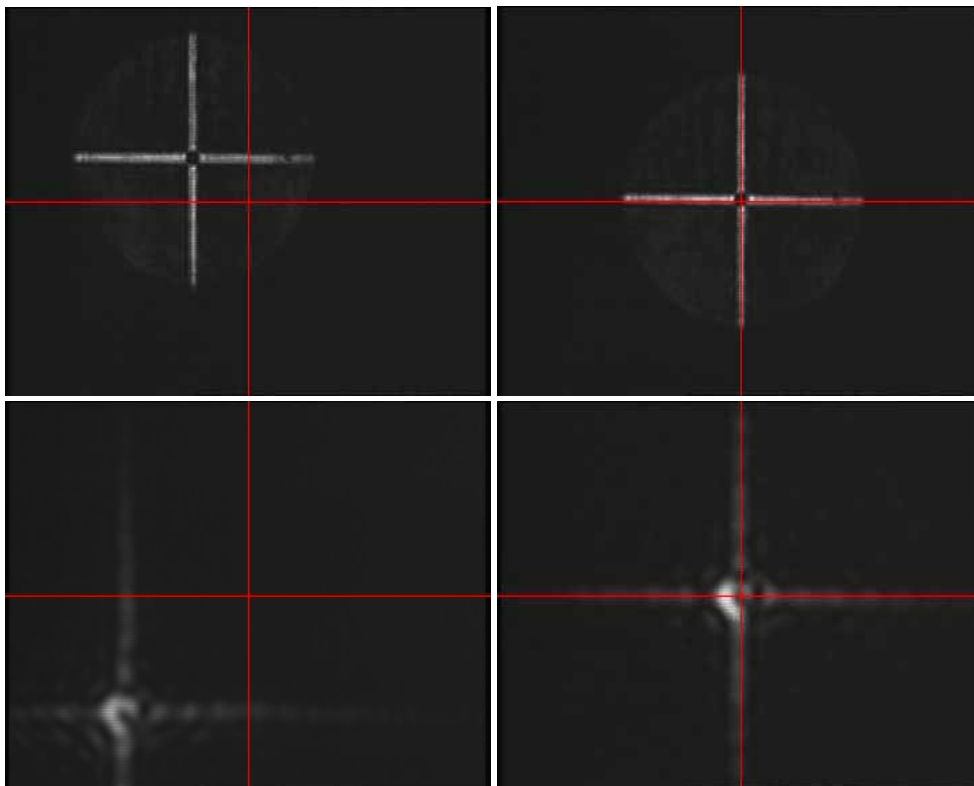


Fig. 8. (AVI: 2.3 MB) Movie of beam alignment. The frames above show the focused and defocused crosshairs before and after alignment. In the video we show the alignment being performed, and that the crosshair is indeed aligned. The video is real time, and the alignment of the top beam is completed in less than 20 seconds.

From the movie frames shown in Fig. 8 it is clear that image analysis [13] determining the screen coordinates for the laser crosshair, will be quite simple to implement. Merely searching for the brightest vertical and horizontal line will provide the coordinates for the crosshair to center. To make the alignment fully automated, the computer must also be able to automatically bring the images into focus.

The alignment described above leaves the beams perfectly aligned, with no separation of the two objectives' image planes. To make a stable set of CB traps there must be some separation of these planes [6-8]. This final step is done by the user choosing a separation and the computer subsequently adjusting the position of the lower objective accordingly. To a good approximation (from having vastly different focal lengths f_1 and f_2) the image plane is displaced by the same distance that the objective is moved, except for a factor of the refractive index of the sample medium wherein the image planes are positioned (*e.g.* water). The sample must be moved to a position where the particles to be captured are available. This is easily done by moving the sample up until the particles come into view on the CCD camera.

The sample chamber can also be translated laterally by mouse control, enabling the user to easily search for interesting objects not visible in the immediate field of view. Finally, the

computer turns on both upper and lower beam sets and the laser is set at a suitable intensity for optical trapping.

4. Sample loading system

To allow for easy and safe replacement of samples, we have modified an ordinary CD-ROM drive to act as a sample loading device. A sample is mounted on a disc, which is placed in the drive tray. The sample disc is affixed to the loading tray by metal spikes aligned to small holes in the loading disc.

The CD-ROM drive is modified to keep the loading tray in a fixed position inside the drive, when the drive is closed. The modification consists of tray stops at the back of the drive that force the tray down below them. With these stops, the drive returns the sample to within 5 μm of the original position after an open-close cycle. The entire drive is mounted on the computer-controlled sample stage, allowing the user to precisely position the sample at the desired location. The CD-ROM drive has holes cut through the top and bottom and some electronics has been removed, permitting the laser beams to access the sample. The current implementation of the sample loading system is illustrated in Fig. 9.

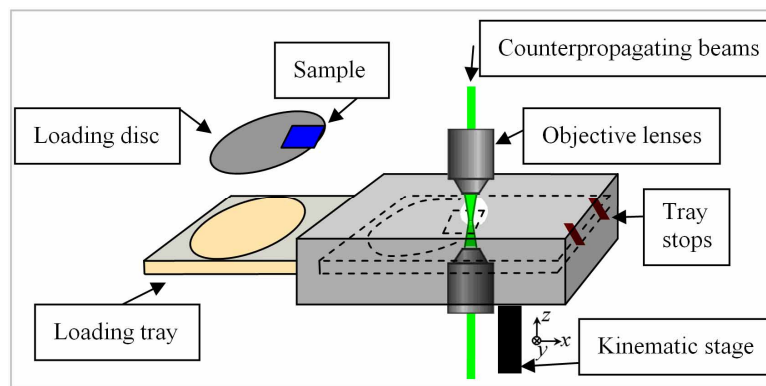


Fig. 9. CD-ROM drive customized to work as sample loading system. The large working distance between objective lenses and the absence of high-NA immersion liquid, allow for the insertion of an automated sample loading device as demonstrated.

The inclusion of a loading tray removes the remaining direct user interaction with the optical hardware, resulting in added stability of the optical setup, ease-of-use, as well as laser safety precautions.

5. Conclusion

We have shown that, by integrating computer-controlled mirror mounts, sample stage, and objective holder, we can simplify the calibration procedure to a few quick steps of mouse-dragging an image to the center position of a computer screen. This GUI-assisted drag-and-drop calibration procedure allows a user to intuitively align the beams in less than one minute. Previously, using manual adjustments of mirrors this process took considerably longer, and required technical skills and experience with optical instrumentation. By implementing actuators on one objective lens, we have also gained precise control of the separation of focal planes necessary for creating stable CB traps.

In addition, a user no longer needs to directly interact with the optical hardware. This makes the system safer to operate in particular for inexperienced users. By implementing an automated loading tray, which is able to load and eject the sample, all user interaction can be done in a safe distance from the optical beam path. Since our system does not require oil immersion and can have a large working distance between objectives, such a loading tray is simple to devise and integrate with the motorized sample holder.

By the improvements described here, we have resolved important issues for creating a user-friendly 3D real-time multi-beam optical trapping system.

Acknowledgments

We would like to thank the support from the EU-FP6-NEST program (ATOM3D), the ESF-Eurocores-SONS program (SPANAS) and the Danish Technical Scientific Research Council (FTP).